Advances in Brief

Inhibition of Glioma Angiogenesis and Growth *in Vivo* by Systemic Treatment with a Monoclonal Antibody against Vascular Endothelial Growth Factor Receptor-2[1]

Philip Kunkel, Ulrike Ulbricht, Peter Bohlen, Marc A. Brockmann, Regina Fillbrandt, Dimitrios Stavrou, Manfred Westphal, Katrin Lamszus[2]

Departments of Neurosurgery [P. K., U. U., M. A. B., R. F., M. W.] and Neuropathology [D. S., K. L.], University Hospital Hamburg-Eppendorf, 20246 Hamburg, Germany, and ImClone Systems, Inc. [P. B.], New York, New York 10014

Abstract

Using an orthotopic intracerebral model, we investigated whether systemic treatment with DC101, a monoclonal antibody against vascular endothelial growth factor receptor (VEGFR)-2, could inhibit angiogenesis and the growth of human glioblastoma cells in severe combined immunodeficient mice. Intraperitoneal treatment with DC101, control IgG, or PBS was initiated either on day 0 or, in another series, on day 6 after tumor cell implantation, and animals were killed ~2 weeks after tumor cell injection. Tumor volumes in animals treated with DC101 were reduced by 59 and 81% compared with IgG and PBS controls, respectively ($P < 0.001$), when treatment was initiated immediately, and similar results were obtained when treatment started on day 6. Microvessel density in tumors of DC101-treated animals was reduced by at least 40% compared with animals treated with control IgG or PBS ($P < 0.01$). We observed a reduction in tumor cell proliferation and an increase in apoptosis in DC101-treated animals ($P < 0.001$). However, in mice treated with DC101, we also noticed a striking increase in the number and total area of small satellite tumors clustered around, but distinct from, the primary. These satellites usually contained central vessel cores, and tumor cells often had migrated over long distances along the host vasculature to eventually reach the surface and spread leptomeningeally. We conclude that systemic antagonization of VEGFR-2 can inhibit glioblastoma neovascularization and growth but can lead to increased cooption of preexistent cerebral blood vessels. Therefore, a combination of different treatment modalities which also include anti-invasive therapy may be needed for an effective therapy against glioblastoma, and the use of an antibody against VEGFR-2 may be one effective component.

Introduction

Over the past decades there have been only minor improvements in the prognosis for patients with glioblastomas. Because glioblastomas as well as virtually all other tumors require angiogenesis to sustain growth, and malignant gliomas have been shown to be among the most densely vascularized tumors (1), antagonization of angiogenesis might be a promising treatment strategy. VEGF[3] is a crucial mediator of glioblastoma angiogenesis. It is secreted by the tumor cells and acts on the endothelial cells, which express the receptors VEGFR-1 (Flt-1) and VEGFR-2 (Flk-1/KDR; Ref. 2). Whereas VEGFR-2 seems to mediate the major growth and permeability actions of VEGF,

VEGFR-1 may act either as a decoy receptor or by suppressing signaling through VEGFR-2 (3). In malignant gliomas VEGF is preferentially expressed around necrotic (hypoxic) areas (2), and levels of VEGF protein as well as mRNA correlate with the malignancy grade and microvessel density of gliomas (4, 5).

Previously, the interaction between VEGF and its receptors has been antagonized by monoclonal antibodies, expression of a dominant-negative receptor or antisense, and by small molecules, thereby inhibiting the growth of glioma xenografts in a variety of rodent models (6–11). Recently it was described that DC101, a mAb against mouse VEGFR-2 (12), could potently inhibit the angiogenesis and growth of several different s.c. tumor xenografts, including human glioblastomas, in nude mice (6). However, when evaluating antiangiogenic strategies in animal models, one must consider that the morphology, function, and antigen expression pattern of the tumor vasculature is largely dependent upon the host environment (13, 14). Therefore, and also because gliomas in contrast to peripheral tumors tend to migrate over long distances, preferably along preexistent cerebral blood vessels, any experimental strategy directed against gliomas should best be evaluated in an orthotopic model. For this reason, we treated glioblastomas grown intracerebrally in SCID mice with DC101 and determined its effect on tumor size and vascularity as well as the proliferative activity and apoptosis *in vivo*.

Materials and Methods

Antibodies. The rat mAb DC101 against mouse VEGFR-2 (12) was provided by ImClone Systems, Inc. (New York, NY). Control polyclonal rat IgG was purchased from Jackson ImmunoResearch Laboratories (West Grove, PA). mAb A4.6.1 against VEGF was a kind gift of Dr. Napoleone Ferrara (Genentech, Inc., San Francisco, CA). The polyclonal antibody against vWF and the mAb MIB-1 against the Ki-67 antigen were obtained from Dako (Hamburg, Germany).

Cell Culture. G55 cells that had previously undergone one round of *in vivo* selection in nude mice were grown in DMEM with 10% FCS. For animal experiments, cell inoculum consisted of the desired number of cells in 5 μl of serum-free tissue culture medium supplemented with 2% methyl cellulose (Sigma Chemical Co., St. Louis, MO).

Orthotopic Glioma Model. Intracerebral G55 xenografts were established following a protocol by Dr. Yancey Gillespie (15). Female SCID mice (C.B.-17 *scid/scid*), 11–12 weeks of age, were anesthetized by i.p. administration of ketamine (100 mg/kg body weight) and xylazine (5 mg/kg body weight). A midline scalp incision was made, and a 0.5-mm burr hole was drilled in the skull 1.5 mm to the right of the midline and 0.5 mm anterior to the bregma. Tumor cells (7×10^4 cells/dose) were loaded into a 250-μl Hamilton syringe fitted with a 30-gauge 0.5-inch needle, attached to a repeating dispenser, and mounted in a stereotaxic holder (TSE Systems, Bad Homburg, Germany). The needle was inserted vertically through the burr hole to a depth of 2.5 mm. After injection of 5 μl of cells into the right caudate nucleus, the needle was withdrawn after 2 min, the burr hole was tamped with bone wax, and the skin was closed with wound clips. The first group of mice were treated i.p. with the mAb DC101 (800 μg/dose in 200 μl PBS), control rat IgG (800 μg/200 μl), or PBS only (200 μl), starting on the day of tumor cell

injection, every other day over a total of 16 days. The experiment was repeated with a modified schedule, where mice received injections of DC101, control IgG, or PBS in the same doses, but treatment was initiated on day 6 of the experiment, and mice were killed on day 15 using CO_2.

Determination of Tumor Size. Mouse brains were removed from the cranial cavity, bisected coronally at the injection site, embedded in OCT compound (Tissue Tek, Elkhart, IN), and stored in liquid nitrogen. Serial frozen sections (12 μm thick) were stained with H&E. The maximum cross-sectional area of the intracranial glioblastoma xenografts as well as the area of smaller satellite tumors distinct from the primary was determined by computer-assisted image analysis. The tumor volume was estimated with the formula: volume = (square root of maximal tumor cross-sectional area)^3.

Determination of Microvessel Density, Proliferative Activity, and Apoptosis. For immunohistochemistry, frozen sections were fixed in acetone and blocked in methanol with 0.3% peroxide. To stain microvessels, sections were incubated with an antibody against vWF (1:200) overnight at 4°C, and bound antibody was detected using the Vectastain kit (Vector Laboratories, Burlingame, CA). Vessel density was determined by computer-assisted image analysis (Quantimed 500; Leica, Hamburg, Germany), measuring the percentage of tumor cross-sectional area consisting of blood vessels in the most densely vascularized area of each tumor and averaging over three hpfs. To analyze the proliferative activity, sections were immunostained with an antibody against the Ki-67 antigen using the Vectastain kit. The fraction of MIB-1 positive nuclei (MIB-1 labeling-index) was determined by counting tumor cell nuclei in three randomly selected hpfs (0.031 mm^2 each). In addition, the number of mitoses was counted in five randomly selected hpfs of each tumor. To detect apoptotic cells, *in situ* end labeling was performed after fixation of the sections in 4% paraformaldehyde, using the *in situ* apoptosis detection kit from Roche (Mannheim, Germany) with 3′3-diaminobenzidine (Sigma Chemical Co.) as substrate.

***In Situ* Hybridization.** Digoxigenin-labeled antisense and sense riboprobes were generated by *in vitro* transcription from a cDNA encoding human $VEGF_{165}$ (16) using T3 (antisense) or T7 (sense) RNA polymerases and the DIG RNA labeling kit (Roche). Frozen sections (12 μm) were fixed in 4% paraformaldehyde, dehydrated, digested with Proteinase K (10 μg/ml; Sigma Chemical Co.), postfixed in 4% paraformaldehyde, acetylated, and dehydrated. Sections were prehybridized in 50% deionized formamide, 5× hybridization salts [750 mM NaCl, 25 mM PIPES (pH 6.8), 25 mM EDTA, 5× Denhardt's solution, 0.2% SDS, 10 mM DTT, 250 μg/ml denatured herring sperm DNA (Sigma Chemical Co.), and 250 μg/ml yeast tRNA (Life Technologies, Inc.)] at 68°C for 1.5 h. Hybridization was carried out at 68°C overnight with the labeled $VEGF_{165}$-riboprobe at 0.5 μg/ml in prehybridization buffer plus 10% dextran sulfate. Slides were washed twice in 0.2× SSC at 68°C for 30 min. Hybridization was detected using an alkaline phosphate conjugate antidigoxigenin antibody (Roche) with NBT/BCIP as substrate according to the manufacturer's instructions.

Western Blot Analysis. Tumors derived from G55 cells grown intracerebrally were lysed with ice-cold 20 mM Tris-HCl (pH 7.4) containing protease inhibitors. Lysates (100 μg of protein) were separated on a 12% polyacrylamide gel under reducing conditions and blotted onto an Immobilon-P membrane (Millipore Corp., Eschborn, Germany). Blots were blocked with 5% nonfat dry milk in PBS containing 0.2% Tween 20 and incubated with anti-VEGF mAb A4.6.1 (1:200) overnight at 4°C. After washing, filters were incubated with a rabbit antimouse antibody conjugated with horseradish peroxidase (Dako) at room temperature for 20 min. The blot was developed with enhanced chemiluminescence reagents (Amersham, Arlington Heights, IL).

Modified Boyden Chamber Migration Assay. The effect of DC101 on the motility of glioblastoma cell line G55 was analyzed using a modified Boyden chamber assay as described previously (17). Antibody DC101 was diluted in cell culture medium and added to the lower wells of a 96-well modified Boyden chamber (Neuroprobe, Cabin John, MD) in concentrations ranging from 0.1 ng/ml to 50 μg/ml. Wells were covered with an 8-μm pore size Nucleopore filter coated with Vitrogen 100 (Collagen, Fremont, CA). Triplicates of G55 cells were seeded into the upper wells at 1.5×10^4 cells in 50 μl of culture medium. After a 5-h incubation at 37°C, migrated cells were stained with Diff-Quick (Dade, Unterschleissheim, Germany), and the nuclei were counted in 10 high-power fields using a ×40 objective with a calibrated ocular grid.

Proliferation Assay. G55 cells were seeded into a 96-well plate (2000 cells/well), and incubated in 200 μl of serum-free medium in the presence or absence of DC101 in six different concentrations ranging from 0.5 ng/ml to 5 ng/ml for 5 days. The culture medium was replaced every other day, and quadruplicate cell counts were determined every day.

Methods of Data Analysis. Differences between tumor volumes, vessel densities, numbers of satellite tumor nodules, numbers of mitoses, MIB-1 indices, and apoptotic indices were analyzed using the unpaired t test or the Mann-Whitney rank-sum test.

Results

VEGF Expression *in Vivo*. For *in vivo* experiments we used the glioblastoma cell line G55, which secretes VEGF *in vitro* (not shown). Stereotactic injection of 7×10^4 G55 cells into the basal ganglia of SCID mice resulted in a 100% tumor take rate. In these tumors, VEGF expression was demonstrated by Western blot and *in situ* hybridization analysis (Fig. 1, *A–C*). Histologically, the tumors resembled human glioblastomas, displaying pseudopalisading necroses and hypervascularity.

Tumor Growth *in Vivo*. In the first set of experiments, treatment with DC101, control IgG, or PBS was initiated on the day of the tumor cell implantation and continued over a total of 16 days. The mean tumor volume in DC101-treated animals was reduced by 59% compared with IgG controls (2.92 ± 0.82 mm^3 *versus* 7.16 ± 2.01 mm^3, respectively; $P < 0.001$), and by 81% compared with PBS controls (15.41 ± 6.133 mm^3; $P < 0.001$); notably, the size of tumors in IgG-treated mice was also reduced by 54% compared with PBS controls ($P < 0.01$; Fig. 1, *D–F* and Fig. 2*A*). In the repeat experiment, treatment was initiated on day 6 after tumor cell injection to investigate whether DC101 treatment was also effective against already-established tumors. From pilot experiments we knew that tumors reached a size of ~1 mm^3 after 6 days and usually would have killed the animals at ~3 weeks of growth. By the end of this second experiment, the mean tumor volume in mice treated with DC101 was reduced by 72% compared with IgG controls ($P = 0.001$), and by 81% compared with PBS controls ($P < 0.001$; not shown). In contrast with the first set of experiments, tumors in the IgG control group were not significantly smaller than tumors in the PBS control group ($P = 0.751$).

Tumor Morphology. We observed a strikingly more invasive pattern of tumor growth in mice treated with DC101 compared with both control groups. Glioblastoma xenografts usually grow as relatively well-circumscribed masses when injected into the caudate/putamen of SCID mice (Fig. 1*G*); however, in DC101-treated animals, a striking increase in the number of satellite tumor that were clustered around, but distinct from, the primary was observed (Fig. 1*H*). These satellites usually contained discernible central vessel cores (Fig. 1*I*). On some sections, it became evident that the satellites represented cross sections of vessels that were surrounded over a long distance by a coat of tumor cells (Fig. 1*J*). Sometimes, such vessels even could be traced to the brain surface, so that, apparently, tumor cells had migrated in the Virchow-Robin space to eventually reach the meninges and spread in the subarachnoid space (Fig. 1*K*). Quantification of tumor satellites revealed that, in the first set of experiments, their frequency was ~5.5-fold greater in the DC101-treated animals than in either IgG- or PBS-controls ($P < 0.01$; Fig. 2*B*). The total satellite tumor area was ~4-fold greater in DC101-treated mice than in either IgG- or PBS-controls ($P < 0.05$ and $P < 0.01$, respectively; Fig. 2*C*). Similarly, in the second set of experiments, the number of satellites was 5-fold greater in DC101-treated mice compared with IgG-controls ($P < 0.001$), and 1.7-fold greater than in PBS-controls ($P < 0.05$; not shown). The total satellite tumor area was 4.8-fold greater in DC101-treated animals than in IgG-controls ($P < 0.001$),
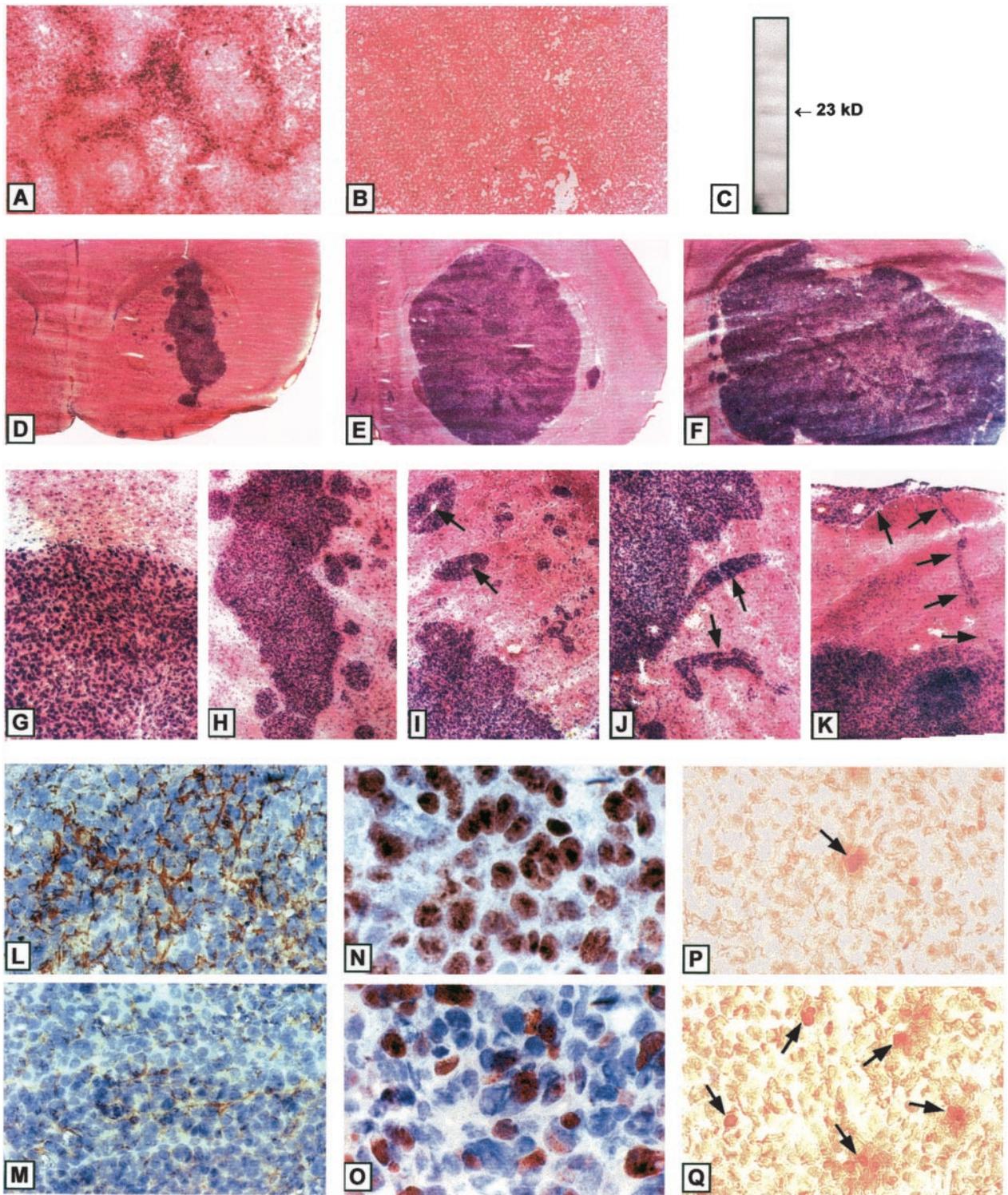
6625

Fig. 1. Examination of tumors in DC101-treated mice and controls. *In situ* hybridization of a tumor derived from cell line G55 grown intracranially in an untreated mouse revealed expression of VEGF mRNA predominantly around necrotic tumor areas (*A,* antisense hybridization; *B,* sense control; both ×40). Western blot analysis of tissue generated from an intracranially grown G55-derived tumor revealed a major band at M_r 23,000 corresponding to the major splice variant $VEGF_{165}$ (*C*). Representative size examples of G55-derived tumors grown intracranially in mice treated with DC101 (*D*), IgG (*E*), or PBS (*F*), (*D–F,* H&E staining, ×10). Whereas tumors in control animals usually displayed well-delineated margins (*G,* example of an IgG-treated tumor), tumors in DC101-treated animals were usually surrounded by numerous smaller satellite tumors (*H*); the satellites usually contained central vessel cores (*I, arrows*); when cut longitudinally, the satellites could be identified as tumor cells migrating along central vessels away from the tumor mass, taking the shape of finger-like protrusions (*J*); occasionally, such finger-like extensions could be traced from the tumor to the cortical surface where tumors cells then spread in the subarachnoid space (*K; G–K,* H&E staining, ×35). Immunostaining for vWF revealed a dense capillary network in control tumors (*L,* IgG-control), but only sparse vascularization in tumors from DC101-treated mice (*M;* both ×170). The average percentage of Ki-67 immunoreactive cells was significantly higher in control tumors (*N,* IgG-control) then in tumors of DC101-treated animals (*O;* both ×375). The percentage of apoptotic cells as determined by TUNEL-staining was lower in control tumors (*P,* IgG-control) than in tumors from DC101-treated mice (*Q;* both ×225).
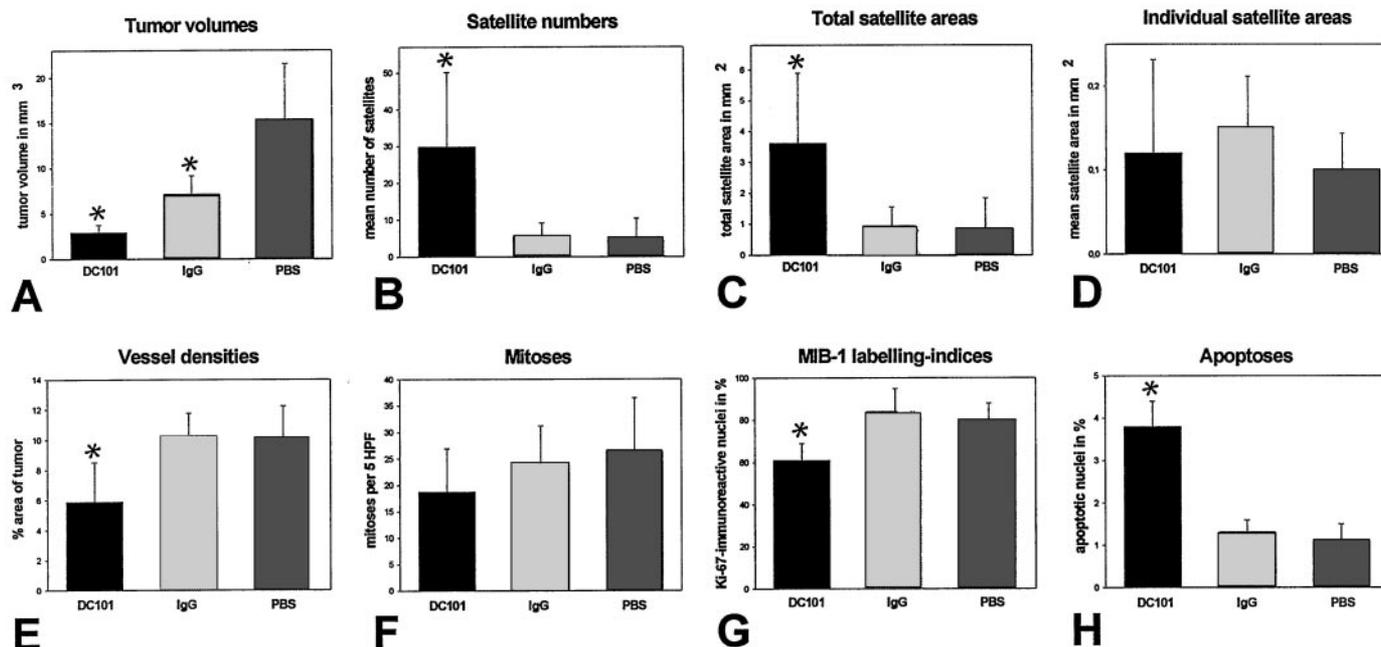
6626

Fig. 2. Comparisons between tumors in DC101-treated mice and tumors in control mice. The mean tumor volume in DC101-treated animals was reduced by 59% compared with IgG-controls and by 81% compared with PBS-controls ($P \leq 0.001$; A). The mean number of tumor satellites surrounding the main tumor mass was ~5.5-fold greater in DC101-treated animals than in either IgG- or PBS-controls ($P < 0.01$; B). The total satellite tumor area was ~4-fold greater in DC101-treated mice than in either IgG- or PBS-controls ($P < 0.05$; C). No significant differences were observed between the mean individual satellite areas in the three treatment groups (D). The mean microvessel density was reduced by ~42% in tumors from DC101-treated mice compared with IgG- and PBS-controls ($P \leq 0.005$; E). Despite a slight tendency toward fewer mitoses in tumors from DC101-treated mice, comparisons with IgG- and PBS-controls did not reach significance ($P > 0.1$; F). The percentage of Ki-67-expressing nuclei was reduced by ~25% in DC101-treated mice compared with IgG- and PBS-controls ($P < 0.001$; G). The fraction of apoptotic nuclei was ~3-fold higher in tumors of DC101-treated animals compared with IgG- and PBS-controls ($P < 0.001$; H). A–F, ∗ indicates significance.

and 2.9-fold greater than in PBS-controls ($P < 0.003$) when treatment was initiated on day 6 (not shown). No significant differences between the mean individual satellite areas were observed between the three treatment groups, regardless of whether treatment was initiated on day 0 (Fig. 2D) or on day 6 (not shown).

Tumor Microvessel Density. Vessel densities were quantified on histological sections after staining for vWF, which specifically labels endothelial cells. In DC101-treated SCID mice, intratumoral microvessel density was reduced by 43 and 41% compared with IgG controls and PBS controls, respectively ($P \leq 0.005$; Fig. 1, L and M, and Fig. 2E). A similar result was obtained when treatment was initiated on day 6 after tumors had established; in this second set of experiments, vessel density was reduced by 50% compared with IgG controls and by 42% compared with PBS controls ($P < 0.01$; not shown). There were no differences in vessel densities between the two control groups.

Tumor Cell Proliferation. The numbers of mitotic figures did not differ significantly between the three treatment groups, although a slight tendency of fewer mitoses in the DC101-treated mice is suggested in Fig. 2F. Results were similar when treatment was initiated on day 6 after tumor cell implantation (not shown). To obtain a more sensitive measure of tumor cell proliferation, we determined the percentage of cells expressing the Ki-67 antigen. In this comparison, differences became more obvious with an ~25%-reduction of proliferative activity in tumors of DC101-treated mice compared with controls ($P < 0.001$; Fig. 1N and O and Fig. 2G). A similar result with an almost 25%-reduced average MIB-1 labeling-index in the DC101 group compared with both controls was obtained when treatment was initiated on day 6 ($P < 0.001$; not shown). No differences were observed between the two control groups.

Notably, DC101 had no effect on the proliferation of G55 cells over 5 days *in vitro* when added at concentrations ranging from 0.5 ng/ml to 5 μg/ml (not shown). Moreover, in a modified Boyden chamber

assay, no effect on the random motility of G55 cells could be observed upon addition of DC101 in concentrations ranging from 0.1 ng/ml to 50 μg/ml (not shown).

Tumor Cell Apoptosis. DC101-treated animals displayed a >3-fold higher percentage of apoptotic tumor cells in comparison with both IgG- and PBS-controls ($P < 0.001$; Fig. 1, P and Q, and Fig. 2H). A similar result was obtained when treatment started on day 6, with an at least 3.5-fold-increased apoptotic rate in tumors of DC101-treated mice compared with both control groups ($P < 0.001$; not shown). There were no differences between the two control groups.

Discussion

The results of this study demonstrate that blockade of VEGFR-2 by systemic administration of DC101 inhibits angiogenesis and growth of human glioblastoma xenografts in an orthotopic model. Antibody treatment was well tolerated; we did not observe any signs of antibody toxicity, and there were no organ abnormalities at autopsy. Tumors volumes in DC101-treated animals were reduced by 59 and by 81% compared with IgG and PBS controls, respectively, when treatment was initiated immediately, and similar results were obtained when treatment started on day 6 after tumor cell implantation. Microvessel density in tumors of DC101-treated animals was reduced by at least 40% compared with animals treated with control IgG or PBS. We did not observe any significant effect of DC101 on glioblastoma cell growth or migration *in vitro*, suggesting that the inhibition of tumor growth *in vivo* is caused by the specific inhibition of tumor angiogenesis through the blockade of VEGFR-2-signaling. Furthermore, we observed a decrease in tumor-cell proliferation and an increase in apoptotic tumor cells in DC101-treated mice, which can be interpreted as a consequence of the lack of new vasculature needed to supply the rapidly growing tumor mass and may also indicate the lack of growth and survival factors produced by the tumor vasculature.

Interestingly, morphological analysis of tumor growth patterns in all experiments consistently revealed a significant increase in the number and total area of satellite tumors clustered around the main tumor mass in DC101-treated animals compared with controls. The satellites usually contained central vessel cores, and tumor cells had often migrated over long distances along these vessels to eventually reach the surface and invade the leptomeninges. Such a pattern of migration is similar to the growth pattern of gliomas in humans, which often invade the brain along the host vasculature in the Virchow-Robin space, so that tumor cell cuffing of vessels in some distance to the main tumor mass is a frequent neuropathological finding. Recently, it has been verified experimentally that gliomas can coopt preexistent cerebral vessels to provide their blood supply before they induce neovascularization (18). Our results suggest that in a therapeutic situation where angiogenesis is inhibited, the two pathways can become alternatives, so that blockade of neovascularization favors vessel cooption. Interestingly, a similar result was obtained using an alternative approach with an antibody against VEGF, where treatment resulted in increased survival in glioblastoma-bearing nude mice compared with PBS controls, but also lead to increased invasiveness along host vessels (8). These findings demonstrate that it is essential to evaluate antiangiogenic therapies in orthotopic models, because angiogenic mechanisms may differ greatly between different organs and tumor types.

Another important finding of our study is that systemic application of DC101 was effective against an intracerebral tumor. A recent study showed that an mAb against a tumor-specific mutant variant of the epidermal growth factor receptor was only effective when applied locally into intracerebral tumors, but not systemically (19). The advantage of DC101 in this comparison is that it only needs to reach the abluminal side of the endothelial cells where VEGFR-2 is mainly located (20), but not to fully cross the blood-brain barrier and diffuse through the brain parenchyma. Interestingly in this context, we also observed an effect of IgG, though by far not as great as that of DC101. A recent study showed that human IgG when injected i.v. into SCID mice reduced the formation of melanoma metastases, and the effect was mainly attributed to an enhancement of natural killer cell activity and interleukin-12 production by mononuclear cells (21), which explains its systemic effect also in our study. The fact that IgG only had a significant effect when treatment was initiated immediately could mean that either IgG is less effective against already established tumors, or that its effect requires more time. It is relatively common to use polyclonal IgG from the same species as the antibody to be tested as a control (6, 22); alternatively, in many studies just saline solution is used (7, 8). Our results demonstrate that when using only polyclonal IgG as a control, effects of any antibody to be tested could be masked to some extent in this comparison.

In summary, we have shown that systemic treatment with an antibody against VEGFR-2 inhibits glioblastoma angiogenesis *in vivo* and leads to a decrease in tumor volume, but at the same time causes an increase in tumor invasiveness along host microvasculature. These findings suggest that a combination of different treatment regimens which also include anti-invasive therapy may be needed for an effective therapy against glioblastoma, and the use of an antibody against VEGFR-2 may be one effective component.

Acknowledgments

References

1. Brem, S., Cotran, R., and Folkman, J. Tumor angiogenesis: a quantitative method for histologic grading. J. Natl. Cancer Inst., *48:* 347–356, 1972.
2. Plate, K. H., Breier, G., Weich, H. A., and Risau, W. Vascular endothelial growth factor is a potential tumour angiogenesis factor in human gliomas *in vivo*. Nature (Lond.), *359:* 845–848, 1992.
3. Yancopoulos, G. D., Davis, S., Gale, N. W., Rudge, J. S., Wiegand, S. J., and Holash, J. Vascular-specific growth factors and blood vessel formation. Nature (Lond.), *407:* 242–248, 2000.
4. Schmidt, N. O., Westphal, M., Hagel, C., Ergun, S., Stavrou, D., Rosen, E. M., and Lamszus, K. Levels of vascular endothelial growth factor, hepatocyte growth factor/ scatter factor and basic fibroblast growth factor in human gliomas and their relation to angiogenesis. Int. J. Cancer, *84:* 10–18, 1999.
5. Samoto, K., Ikezaki, K., Ono, M., Shono, T., Kohno, K., Kuwano, M., and Fukui, M. Expression of vascular endothelial growth factor and its possible relation with neovascularization in human brain tumors. Cancer Res., *55:* 1189–1193, 1995.
6. Prewett, M., Huber, J., Li, Y., Santiago, A., O'Connor, W., King, K., Overholser, J., Hooper, A., Pytowski, B., Witte, L., Bohlen, P., and Hicklin, D. J. Antivascular endothelial growth factor receptor (fetal liver kinase 1) monoclonal antibody inhibits tumor angiogenesis and growth of several mouse and human tumors. Cancer Res., *59:* 5209–5218, 1999.
7. Kim, K. J., Li, B., Winer, J., Armanini, M., Gillett, N., Phillips, H. S., and Ferrara, N. Inhibition of vascular endothelial growth factor-induced angiogenesis suppresses tumour growth *in vivo*. Nature (Lond.), *362:* 841–844, 1993.
8. Rubenstein, J. L., Kim, J., Ozawa, T., Zhang, M., Westphal, M., Deen, D. F., and Shuman, M. A. Anti-VEGF antibody treatment of glioblastoma prolongs survival but results in increased vascular cooption. Neoplasia, *2:* 306–314, 2000.
9. Vajkoczy, P., Menger, M. D., Vollmar, B., Schilling, L., Schmiedek, P., Hirth, K. P., Ullrich, A., and Fong, T. A. Inhibition of tumor growth, angiogenesis, and microcirculation by the novel Flk-1 inhibitor SU5416 as assessed by intravital multi-fluorescence videomicroscopy. Neoplasia, *1:* 31–41, 1999.
10. Saleh, M., Stacker, S. A., and Wilks, A. F. Inhibition of growth of C6 glioma cells *in vivo* by expression of antisense vascular endothelial growth factor sequence. Cancer Res., *56:* 393–401, 1996.
11. Millauer, B., Shawver, L. K., Plate, K. H., Risau, W., and Ullrich, A. Glioblastoma growth inhibited *in vivo* by a dominant-negative Flk-1 mutant. Nature (Lond.), *367:* 576–579, 1994.
12. Rockwell, P., Neufeld, G., Glassman, A., Caron, D., and Goldstein, N. *In vitro* neutralization of vascular endothelial growth factor activation of flk-1 by a monoclonal antibody. Mol. Cell. Differ., *3:* 91–109, 1995.
13. Roberts, W. G., Delaat, J., Nagane, M., Huang, S., Cavenee, W. K., and Palade, G. E. Host microvasculature influence on tumor vascular morphology and endothelial gene expression. Am. J. Pathol., *153:* 1239–1248, 1998.
14. Arap, W., Pasqualini, R., and Ruoslahti, E. Cancer treatment by targeted drug delivery to tumor vasculature in a mouse model [comment in: Science (Wash. DC), *279:* 323–324, 1998]. Science (Wash. DC), *279:* 377–380, 1998.
15. Chambers, R., Gillespie, G. Y., Soroceanu, L., Andreansky, S., Chatterjee, S., Chou, J., Roizman, B., and Whitley, R. J. Comparison of genetically engineered herpes simplex viruses for the treatment of brain tumors in a scid mouse model of human malignant glioma. Proc. Natl. Acad. Sci. USA, *92:* 1411–1415, 1995.
16. Weindel, K., Marme, D., and Weich, H. A. AIDS-associated Kaposi's sarcoma cells in culture express vascular endothelial growth factor. Biochem. Biophys. Res. Commun., *183:* 1167–1174, 1992.
17. Lamszus, K., Schmidt, N. O., Jin, L., Laterra, J., Zagzag, D., Way, D., Witte, M., Weinand, M., Goldberg, I. D., Westphal, M., and Rosen, E. M. Scatter factor promotes motility of human glioma and neuromicrovascular endothelial cells. Int. J. Cancer *75:* 19–28, 1998.
18. Holash, J., Maisonpierre, P. C., Compton, D., Boland, P., Alexander, C. R., Zagzag, D., Yancopoulos, G. D., and Wiegand, S. J. Vessel cooption, regression, and growth in tumors mediated by angiopoietins and VEGF. Science (Wash. DC), *284:* 1994–1998, 1999.
19. Sampson, J. H., Crotty, L. E., Lee, S., Archer, G. E., Ashley, D. M., Wikstrand, C. J., Hale, L. P., Small, C., Dranoff, G., Friedman, A. H., Friedman, H. S., and Bigner, D. D. Unarmed, tumor-specific monoclonal antibody effectively treats brain tumors. Proc. Natl. Acad. Sci. USA, *97:* 7503–7508, 2000.
20. Chiarugi, V., Ruggiero, M., and Magnelli, L. Molecular polarity in endothelial cells and tumor-induced angiogenesis. Oncol. Res., *12:* 1–4, 2000.
21. Shoenfeld, Y., and Fishman, P. γ-globulin inhibits tumor spread in mice. Int. Immunol., *11:* 1247–1252, 1999.
22. Stan, A. C., Nemati, M. N., Pietsch, T., Walter, G. F., and Dietz, H. *In vivo* inhibition of angiogenesis and growth of the human U-87 malignant glial tumor by treatment with an antibody against basic fibroblast growth factor. J. Neurosurg., *82:* 1044–1052, 1995.

Inhibition of Glioma Angiogenesis and Growth *in Vivo* by Systemic Treatment with a Monoclonal Antibody against Vascular Endothelial Growth Factor Receptor-2

Philip Kunkel, Ulrike Ulbricht, Peter Bohlen, et al.

Updated version	Access the most recent version of this article at: http://cancerres.aacrjournals.org/content/61/18/6624

Cited articles	This article cites 21 articles, 7 of which you can access for free at: http://cancerres.aacrjournals.org/content/61/18/6624.full#ref-list-1
Citing articles	This article has been cited by 48 HighWire-hosted articles. Access the articles at: http://cancerres.aacrjournals.org/content/61/18/6624.full#related-urls

E-mail alerts	Sign up to receive free email-alerts related to this article or journal.
Reprints and Subscriptions	To order reprints of this article or to subscribe to the journal, contact the AACR Publications Department at pubs@aacr.org.
Permissions	To request permission to re-use all or part of this article, use this link http://cancerres.aacrjournals.org/content/61/18/6624. Click on "Request Permissions" which will take you to the Copyright Clearance Center's (CCC) Rightslink site.